sustainability

MDPI

Article

Evapotranspiration for Sustainable Land Management Systems

Salah M. Alagele [1,2,*], Stephen H. Anderson [3] and Ranjith P. Udawatta [3,4]

[1] Department of Desertification Combat, College of Agricultural Engineering Sciences, University of Baghdad, Baghdad 00964, Iraq
[2] Department of Sustainable Natural Resource Management, International Center for Biosaline Agriculture (ICBA), Dubai P.O. Box 14660, United Arab Emirates
[3] School of Natural Resources, University of Missouri, 302 Anheuser-Busch Natural Resources Building, Columbia, MO 65211, USA; andersons@missouri.edu (S.H.A.); udawattar@missouri.edu (R.P.U.)
[4] The Center for Agroforestry, University of Missouri, 203 Anheuser-Busch Natural Resources Building, Columbia, MO 65211, USA
* Correspondence: salah.alagele@coagri.uobaghdad.edu.iq

Abstract

Evapotranspiration (ET) is a fundamental process within the water cycle and the agricultural water balance, optimizing resource allocation, maintaining soil health, and enhancing ecosystem resilience to climate change. Because ET represents a primary consumptive use of irrigation on agricultural lands, enhancing water-use efficiency and sustainable water management requires accurate estimation of evapotranspiration to support long-term sustainability and productivity. This study offers an effective means to visualize spatial and temporal patterns of reference evapotranspiration (ETo) across various vegetation management practices. This study examined the impacts of agroforestry buffers (ABs), grass buffers (GBs), biofuel crops in an agroforestry watershed (BCa), and biofuel crops in a grass buffer watershed (BCg) on ETo, compared to a corn (*Zea mays* L.)–soybean (*Glycine max* L.) rotation (RC) for claypan soil in Northern Missouri, USA. The experimental watersheds were located at the Greenley Memorial Research Center, Missouri, USA. Campbell Scientific sensors and Photosynthetically Active Radiation (PAR) smart sensors were installed to measure net radiation, anemometers, humidity, and air temperature. All instruments were mounted on masts at a height of 2 m above ground level in crop, tree, grass, and biofuel areas. Measured meteorological data were recorded hourly from April to October during 2017 and 2018. Daily ETo predictions were calculated using the Penman–Monteith model. These ETo predictions were displayed across the landscape using Python-based GIS for selected dates (each Saturday) for the watersheds. The methodology was implemented using the software programs of Python 2.7.10 and ArcGIS 10.3.1. The results indicated that ETo increased by 11%, 17%, 18%, and 25% in 2017, and by 7%, 9%, 14%, and 20% in 2018 for AB, BCa, BCg, and GB, respectively, compared to RC management. This process may improve soil water recharge in perennial management systems. Accurate estimation of ET in agricultural regions is critical for understanding water balance, hydrological and ecosystem processes, and climate variability. Given that agriculture constitutes the majority of global water consumption, precise ET estimation is particularly significant for sustainable water management, especially in regions experiencing water scarcity. These outcomes may support effective planning and management of agricultural water resources by enabling optimized irrigation and agricultural production.

Keywords: reference evapotranspiration; perennial vegetative management practices; Penman–Monteith model; Python-based GIS; sustainable development

Academic Editor: Xia Li

Received: 3 April 2026
Revised: 16 May 2026
Accepted: 19 May 2026
Published: 21 May 2026

1. Introduction

Evapotranspiration (ET) under various vegetative management practices is a critical determinant in evaluating water balance, irrigation strategies, and groundwater recharge [1]. Comprehensive land management requires a detailed water budget, with particular focus on the ET component [2]. Previous studies indicate that ET acts as a primary bidirectional driver in land–atmosphere systems [3]. ET serves as a key mechanism that accelerates water loss through vegetation greening while also regulating local climate and soil moisture [4]. The prevailing consensus is that increased ET, primarily driven by enhanced vegetation, leads to greater water consumption and, consequently, reduces local water availability, particularly in water-limited regions [5]. Although previous studies have primarily focused on estimating ET in crops, there remains limited understanding of its effects across diverse vegetation systems. The study of ET effects across diverse vegetation (e.g., forests and grasslands) represents a rapidly advancing field that addresses significant gaps in hydrological modeling and water resource management [6]. A clear understanding of soil water use in integrated vegetation management systems is essential for addressing significant climate change impacts, such as higher temperatures, increased evaporation, altered rainfall patterns, and changes in growing season length [7]. Therefore, assessment of ET is essential for optimizing water-use efficiency, minimizing excessive irrigation, and protecting water resources [8].

ET includes both evaporation from the land surface and transpiration from plant leaves to the atmosphere [9]. These processes occur simultaneously and are influenced by climate variables, including solar radiation, air temperature, wind speed, and relative humidity [10]. The primary types of ET include actual evapotranspiration (ETa), which represents the water loss under existing moisture conditions, potential evapotranspiration (ETp) refers to water evaporation from a surface with unlimited water, such as a lake, and reference evapotranspiration (ETo) is the rate of water vapor released from a well-watered grass surface.. These definitions of ET provide a standard reference for comparing evapotranspiration values across different regions within a specific area. Typically, the ETa from various crops does not equal the ETp [11]. However, for close-growing crops, maintaining optimal soil moisture for maximum yields generally results in ETa being nearly equal to, or a consistent fraction of, ETp during the active growth phase [12]. Consequently, accurate estimation of hourly or daily evapotranspiration (ET), a complex aspect of agricultural water management, is essential for analyzing soil–plant–water relationships and conducting hydrological studies [13].

Reliable ET estimation is also necessary for drought monitoring, hydrological model validation, and weather forecasting [14]. Given that irrigation water often falls short of meeting total agricultural demand, precise determination of crop water requirements is vital for effective management and conservation of agricultural water resources [15,16]. Accurate assessment of crop water demand depends on precise ET estimation [17]. Koech and Langat [18] emphasize the need for water-efficient technologies and practices to achieve sustainable agricultural water resources. Blatchford [19] identifies crop water productivity as a key metric, evaluated using digital technologies, to assess water-use efficiency in agriculture. Precision agriculture involves monitoring, measuring, and responding to crop variability to reduce cultivation costs, optimize resource use, and enhance efficiency by collecting real-time data from sensors on farm machinery [20]. In semi-arid and arid regions, precision agriculture applications have the potential to enhance the efficiency of irrigated agriculture amid water scarcity and climate change. Both climate change and water scarcity are widely acknowledged as significant risks to sustainable development, affecting the environment, food security, economic activities, and natural resources [14].

Soil and water resources face increasing threats from global population growth and are subject to degradation from both anthropogenic and natural factors [21]. Therefore, conserving soil and water resources is vital to the long-term sustainability of agriculture and the environment [22]. Conservation buffer systems represent a significant practice for resource conservation and warrant broader implementation [23]. Soil water use and storage differ among conservation vegetation systems, influencing land productivity and hydrological processes [24,25]. Soil water content regulates essential processes such as infiltration, redistribution, percolation, evaporation, and plant transpiration [22]. In agricultural production systems, maintaining sufficient soil water is crucial for optimizing crop productivity [26,27]. Integrating trees, grasses, and crops into agroforestry or grass buffer systems can enhance water transpiration and is recognized as a valuable strategy in sustainable agriculture [28]. However, resource competition, particularly for water, from perennial vegetative management systems may reduce crop yields, especially near tree and crop borders [29,30]. Addressing these challenges has led to efforts to improve soil quality, reduce soil erosion, surface runoff, and nutrient and sediment losses, support sustainability, enhance environmental quality, mitigate global climate change, and increase productivity [25,31].

Few studies have examined how vegetative management systems influence ETo and the consequences for ecosystem services. Research by [32] and [33] indicates that buffer systems and nearby areas have reduced energy levels, lowering ET and likely boosting soil water storage. In the same watershed as this study, the study [34] was focused on two buffer cropping systems, specifically agroforestry and grass buffers, to estimate soybean crop ET using the Penman–Monteith equation. In that study, daily averages of meteorological variables were collected over 54 days during the summer of 2007. In contrast, this study is unique in the objectives and methodology. It presents a method for visualizing spatial and temporal patterns of ETo across five vegetation management practices using Python-based GIS. Meteorological data, including temperature, humidity, wind speed, and solar radiation, were collected at regular intervals over seven months, from April to October, in 2017 and 2018. However, researchers in study [34] reported that wind speeds were consistently lower in the agroforestry buffer, with an average reduction of 0.42 m s^{-1} compared to the grass buffer. Furthermore, the study [34] demonstrated that under water-stressed conditions, the decrease in wind speed resulting from agroforestry buffers was nearly offset by a corresponding increase in net radiation. The greatest differences in net radiation between the agroforestry and grass systems occurred in the morning, reaching approximately 40 W m^{-2}, likely due to solar radiation scattered by the agroforestry buffers. The reduction in wind speed over the crop area surrounded by agroforestry buffers depended on wind direction. The study [34] concluded that management of perennial vegetation alters the microclimate, which in turn affects ET, soil water content, and carbon sequestration. This research also showed that agroforestry areas had higher temperatures and net radiation but lower wind speeds than grass watersheds. Both studies demonstrate that buffer orientation relative to the prevailing wind significantly reduces ET.

Several studies reported that tree buffers in alley cropping can act as wind barriers, modifying ET and other energy flows [35,36]. Buffers and perennial systems also increase thermal capacity, reducing heat flow and helping crops adapt to climate challenges [37]. Additionally, the study [38] showed that tree buffers can alter the radiation budget in row crops by altering scattered shortwave and emitted longwave radiation. Models incorporate heat flow, solar radiation, wind speed, and humidity to estimate ETo variability [39]. For example, Ref. [40] applied a Python-based GIS to analyze ET's spatial and temporal variation, demonstrating that this approach simulates ET across diverse land covers, soil textures, water contents, precipitation, and temperature. Mohammed and

https://doi.org/10.3390/su18105209

Trauth [40] conducted a study involving two vegetation systems, specifically deciduous forest and miscellaneous woody area vegetation, in addition to wetlands in Linn County, Missouri. While prior research [40] has primarily focused on estimating ET in crops, there is still limited understanding of ET dynamics across diverse vegetation systems. Thus, this study introduces a novel approach for visualizing spatial and temporal patterns of ETo across five vegetation management practices using Python-based GIS.

Python-based geographic information systems (GIS) can efficiently model ET for a variety of conservation vegetative management systems, and this approach utilizes spatial data to enhance water resource management and assess the effectiveness of conservation measures [41]. Python is widely regarded as the primary scripting language for ArcGIS due to its flexibility in developing new applications and code [42]. Python scripts enable the creation of diverse applications and are essential for extending ArcGIS functionality [43]. This methodology supports advanced spatial analysis, custom tool development, and robust data management, thereby enhancing efficiency in water resource and irrigation management [44]. The primary justifications for employing Python GIS in ET assessment include automation and reproducibility, access to specialized libraries, integration with diverse data sources, enhanced efficiency, and advanced capabilities for visualization and analysis [45]. In general, Python-based GIS tools are better suited for large-scale, complex spatial modeling due to their automation, reproducibility, and ability to manage large datasets. In contrast, Excel is more effective for quick, interactive analysis and ad hoc modeling of small, tabular, non-spatial data. Mohammed and Trauth [40,46] demonstrated that the Python-based GIS effectively visualizes spatial and temporal patterns of estimated ET across multiple vegetation management systems. Their findings indicate that Python scripts are valuable for analyzing geographic conditions and supporting policy and management decisions in various vegetation management contexts. Additionally, a study by [40] developed a GIS-based methodology to compute infiltration across landscapes, accounting for spatial and temporal variability, using the Python Green–Ampt Infiltration Script (GAINS). This approach builds on the foundational infiltration research of Green and Ampt and uses readily available data sources for the required inputs. The Python script produces spatial visualizations of the Green–Ampt infiltration module, which can be displayed in ArcGIS. The authors emphasize that Python-based GIS can accurately estimate soil water processes, such as infiltration and ET, to calculate soil water content, which varies across different conservation management systems. This Python-based GIS methodology represents significant progress toward a unified decision-making tool for wetland mitigation sites and vegetation management systems.

This study presents a novel methodology for estimating ET across multiple vegetative management systems. The spatial distribution map of ETo, generated using a Python-based GIS, identifies water consumption hotspots within the watershed and informs decisions regarding buffer zone spacing and tree species selection [46]. At the policy level, integrating ET indicators into agricultural environmental performance evaluations is recommended [14]. The Python-based GIS developed provides a reliable tool for estimating and visualizing ET across diverse landscapes and management regimes [40,41]. ETo estimates produced by the Python GIS script were consistent with those obtained from Excel-based calculations. Although previous research has primarily focused on estimating ET in crops, there remains limited understanding of its effects across diverse vegetation systems [47]. This study is the first to assess ETo across multiple vegetation systems, including agroforestry buffers (ABs), grass buffers (GBs), biofuel crops, and a corn (*Zea mays* L.)–soybean (*Glycine max* L.) rotation (RC), using the Python-based GIS ET modeling in Knox County, Missouri. The findings offer practical guidance for implementing and managing these vegetation systems, supporting effective planning and addressing key agricultural development challenges. Few studies have been implemented to assess the effects of perennial management systems on ETo using Python-based GIS. This study aimed to evaluate the impacts of long-term sustainable vegetative management systems (AB, BC, and GB) on ETo relative to row crop on claypan soils using Python-based GIS.

Core Ideas

1. The implementation of perennial vegetative management practices enables differential soil water extraction, thereby reducing water and nutrient runoff, and has become essential for sustainable agricultural production systems.
2. Alterations in the microclimate caused by perennial vegetation management systems can influence evapotranspiration, soil water dynamics, carbon sequestration, and related processes.
3. Numerous land management practices necessitate evaluation of the water budget, with particular emphasis on the evapotranspiration component.
4. Python-based GIS have demonstrated efficiency in visualizing spatial and temporal patterns of estimated evapotranspiration across various vegetation management systems.

2. Materials and Methods

2.1. Experimental Site

The research was conducted at the University of Missouri Greenley Memorial Research Center, located in Knox County near Novelty, Missouri, USA (40° 01′ N, 92° 11′ W; Figure 1). Over the past 30 years, the site has received a mean annual precipitation of 920 mm y^{-1}, with 66% occurring between April and September. The average annual air temperature is 11.7 °C, with a mean monthly high of 31.4 °C in July and a mean monthly low of −6.6 °C in February. The average annual snowfall is approximately 590 mm y^{-1} [48].

Three adjacent north-facing watersheds were established in 1991 (Figure 1). The control watershed, located in the east and measuring 1.65 ha, was designated in 1991 and managed using a corn (*Zea mays* L.) and soybean (*Glycine max* L.) rotation (RC) under no-till practices. During the study period, corn and soybeans were planted on 15 April 2017 and 20 May 2018, and harvested on 30 September 2017 and 15 October 2018, respectively. Terrain effects were not considered in this study because the slopes in all three watersheds were uniformly low (approximately 2%).

The grass buffer (GB, west watershed) and agroforestry buffer (AB, center watershed) represent the other two watersheds in this study. Specifically, the GB watershed encompasses 3.16 ha and contains grass-only buffers, whereas the AB watershed covers 4.44 ha and incorporates both grass and tree buffers. The GB treatment consists of five grass buffers. In 1997, a combination of Redtop (*Agrostis gigantea Roth*), bromegrass (*Bromus inermis Leyss*.), and birdsfoot trefoil (*Lotus corniculatus* L.) was established in 4.5 m wide strips, spaced 36.5 m apart, on both the GB and AB watersheds. To characterize vegetation development, the average vegetation height in the GB treatment ranged from 1 to 1.5 m during 2017 and 2018. For the AB watershed, in November 1997, pin oak (*Quercus palustris Muenchh*.), swamp white oak (*Quercus bicolor Willd*.), and bur oak (*Quercus macrocarpa Michx*.) seedlings were planted at 3 m intervals within the grass–legume strips across the six buffers of the AB watershed. By May 2017 and 2018, trees in the AB treatment had reached heights of 8–10 m and exhibited fully developed leaves. Between the buffers on both the GB and AB watersheds, corn–soybean rotations were implemented using a no-till system beginning in 1991. Subsequently, these areas transitioned to biofuel crops (BCs) in 2012. The biofuel seed mix, which included switchgrass (*Panicum virgatum* L.) and winter peas (*Pisum sativum* subsp. *arvense*), was planted between the buffers in 2012. The average vegetation height in the BC treatment was 1–1.5 m in 2017 and 2018. The BC was harvested as forage every June, with occasional additional harvests in September. For this study, the BC treatment included locations within both the GB (BCg) and AB (BCa) watersheds. The perennial vegetative systems of AB, GB, and BC were selected as representative sustainable management practices to compare their effects on ET with those of traditional RC and to evaluate their potential contributions to sustainable land management. These perennial systems primarily improve soil water dynamics, providing effective and sustainable alternatives to traditional RC while enhancing ecosystem services, particularly in degraded agricultural landscapes. Through the development of deep root systems, they increase infiltration and water storage, improve nutrient cycling, reduce greenhouse gas emissions, and promote carbon sequestration.

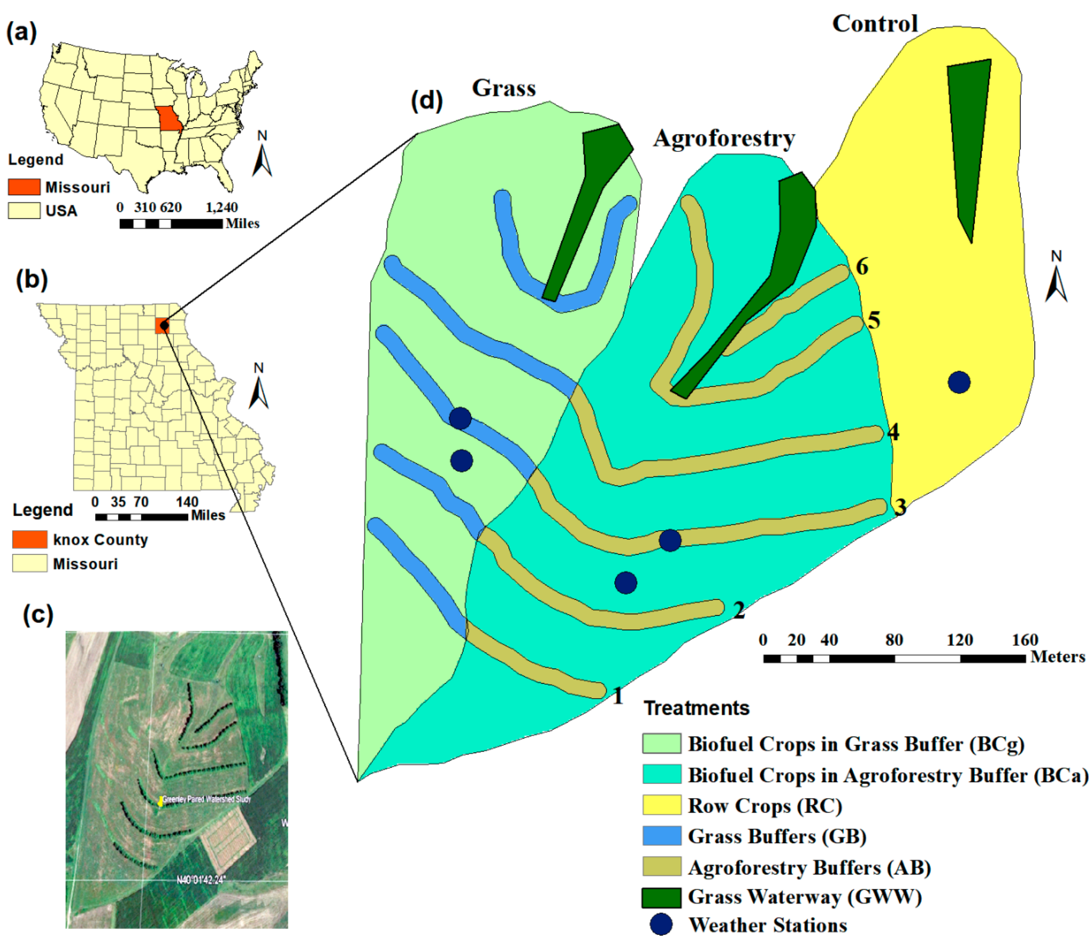

Figure 1. (**a**) Missouri within the United States, (**b**) study site location in University of Missouri Greenley Memorial Research Center in Knox County near Novelty, (**c**) aerial view, and (**d**) land management maps for the grass buffers (west watershed), agroforestry buffers (central watershed) and control (corn–soybean rotation, east watershed) watersheds. All three watersheds have grass waterways at the downslope end of each watershed. Areas between the grass and agroforestry buffers have been managed with biofuel crops since 2012. Dark blue circles represent the weather sensor locations within treatments.

Soils in the three watersheds were mapped according to landscape features and classified as Putnam silt loam (fine, smectitic, mesic Vertic Albaqualfs) and Kilwinning silt loam (fine, smectitic, mesic Vertic Epiaqualfs). The parent materials of these soils consist of glacial till and loess. Both Putnam and Kilwinning soils possess a drainage-restrictive B horizon with a claypan at variable depths ranging from 4 to 37 cm [31], and these soils are found in the Midwest USA (primarily in Missouri). Additional details regarding soils, conservation management practices, and climate are available in Veum et al. [49].

2.2. Microclimate Stations and Data Collection

Temperature, humidity, and wind speed were measured with Campbell Scientific sensors, and net radiation was estimated using Photosynthetically Active Radiation (PAR) (S-LIA-M003) smart sensors. Campbell Scientific and PAR sensors were manufactured by Campbell Scientific Inc., Logan, UT, USA and HOBO® Data Loggers (LI-COR® Brand), USA, respectively. The sensors were mounted on masts positioned 2 m above ground level in the AB, BCa, BCg, GB, and RC treatment areas to estimate ETo. The PAR smart sensor operates over a range of 0 to 2500 $\mu mol/m^2/s$ and wavelengths from 400 to 700 nm. These sensors are compatible with HOBO stations. The PAR values in $\mu mol/m^2/s$ were converted to W/m^2 by dividing by approximately 4.57 for sunlight. Subsequently, net radiation in the FAO-56 PM equation was expressed in megajoules per square meter per day ($MJ/m^2/day$) by multiplying the W/m^2 value by 0.0864. These sensors were connected to dataloggers (CR-23X-4; Campbell Scientific Inc., Logan, UT, USA) to continuously collect weather data at 1 h intervals during the growing season for seven months (April to October) in 2017 and 2018 across all treatments. Five microclimate stations were established in the study areas. Each station had two sensor locations, each equipped with three sensors, for a total of six weather sensors. Two stations were positioned in the third buffer for the GB and AB treatments (Figure 1). For the BC treatment, two microclimate stations were in the grass watershed (BCg) and the agroforestry watershed (BCa); both stations were situated between the second and third buffers in the GB and AB watersheds (Figure 1). One station was installed in the control watershed to collect data for the RC management. All sensor locations were situated in areas with identical slopes, which were uniformly low (approximately 2%) in all three watersheds. Weather data, including temperature, relative humidity, net radiation, and wind speed, were collected over seven months, from April to October, in both 2017 and 2018. These data were downloaded weekly on Saturdays. The data were compiled and presented as weekly estimated ETo to facilitate visualization of the spatial and temporal distribution of ETo within the study area. Several challenges were encountered during data collection (2017 and 2018) from climatic sensors for the assessment of ETo across various management systems in the field. These included harsh environmental conditions that may cause physical damage or fouling, limited connectivity in remote locations, high maintenance costs, and calibration difficulties. In general, limitations of climatic data availability involve significant gaps in spatial and temporal coverage, poor data quality in developing regions, and high costs associated with accessing or digitizing historical records. These constraints often lead to uncertainties in climate modeling and reduce the ability to accurately assess regional risks or validate global climate models. Thus, the availability of high-quality climatic data provides significant advantages for enhancing global resilience and advancing scientific progress by supporting effective climate risk management, informed decision-making, and sustainable resource planning.

2.3. Evapotranspiration Estimation

Daily predictions of ETo were calculated using the Penman–Monteith equation [50], and this requires estimating several parameters.

$$ET_o = \frac{0.408\,\Delta\,(R_n - G) + \gamma \frac{900}{T + 273}\, u_2\,(e_s - e_a)}{\Delta + \gamma(1 + 0.34u_2)} \quad (1)$$

where ETo is the reference evapotranspiration (mm day^{-1}), R_n is net radiation (MJ m^{-2} day^{-1}), G is soil heat flux density (MJ m^{-2} day^{-1}), T is mean daily air temperature at 2 m height (°C), u_2 is wind speed at 2 m height (m s^{-1}), e_s is saturation vapor pressure (kPa), e_a is actual vapor pressure (kPa), Δ is the slope vapor pressure curve (kPa $°C^{-1}$), and γ is the psychrometric constant (kPa $°C^{-1}$). Therefore, the Penman–Monteith equation requires several parameters to solve the formula. These parameters included: (1) temperature (°C), (2) relative humidity (%), (3) wind speed (m s^{-1}), (4) net radiation (MJ m^{-2} day^{-1}), (5) elevation above sea level, which is approximately 750 feet (228.6 m) in Northern Missouri, (6) the latitude of study site, which is 40° 1′45.51″N, (7) albedo or canopy reflection coefficient values according to every single type of vegetation management system (tree, grass, and crop), (8) atmospheric pressure (98.63 Kpa), (9) specific heat at constant pressure (0.001013 MJ kg−1 $°C^{-1}$), (10) latent heat of vaporization (2.45 MJ kg^{-1}), and (11) ratio molecular weight of water vapor (0.622). Albedo values were 0.25 for the BCa, BCg, and GB treatments, 0.15 to 0.18 for trees in the AB treatment, and 0.18 to 0.25 for corn and soybean crops in the RC treatment. Equation (1) was solved according to the procedures detailed in [51], with the corresponding steps provided in the Excel sheet for each treatment (GB, AB, BCg, BCa, and RC).

2.4. Python-Based Geographic Information System (GIS)

The Python script was developed to model and estimate daily ETo using the Penman–Monteith equation for multiple vegetative management systems in 2017 and 2018 in Northern Missouri. The script, executed in the Python 2.7.10, processed input data and generated ETo estimates [42]. ArcGIS version 10.3.1 was used to produce raster maps of ETo for all treatments (GB, BCa, BCg, AB, and RC), assuming each treatment was homogeneous. The methodology employed a Python script to estimate and visualize the spatial and temporal variability of ETo across various landscape patterns using geographic information systems (GIS). Measured weather parameters were used as inputs for ETo computation. The script calculated ETo using Equation (1) for each vegetation management system, and these results were compared with those obtained from a spreadsheet in Excel for each treatment to verify the script's accuracy. The use of the Python script enabled representation of ETo variability over time and space within the study area. Model outputs were presented as GIS raster maps that illustrated spatial and temporal variation for each conservation management practice. Additionally, plots depicting ETo for all treatments over the study period were generated using Python. These visualizations revealed water consumption hotspots within the watershed and could guide the optimization of buffer zone spacing and tree species selection.

2.5. Statistical Analysis

The experimental design implemented at the study site to evaluate the effect of ETo on vegetation management systems over time (weeks) utilized a Randomized Complete Block Design (RCBD) combined with Repeated Measures Analysis. This method manages environmental variability across plots and allows for the observation of changes in ETo within vegetation management systems over several weeks. The General Linear Model (GLM) procedure in SAS (Version 9.4.) was used to assess the statistical significance of estimated total ETo over 27 weeks in 2017 and 2018, calculated using the Penman–Monteith equation [52]. Five treatments were examined: BCa, BCg, AB, GB, and RC. Environmental variables, including temperature (°C), relative humidity (%), wind speed (m s^{-1}), and net radiation (MJ m^{-2} day^{-1}), were recorded using Campbell Scientific and PAR smart sensors. Five microclimate stations were installed in the study area. Each station had two sensor locations, each equipped with three sensors, for a total of six weather sensors per treatment. This configuration was replicated within each treatment. Weather data were collected from April to October in both 2017 and 2018, and no data were missing during the study period. Terrain effects were not considered in this study, as all three watersheds exhibit uniformly low slopes of approximately 2%. Data quality was assessed by examining normality at $p = 0.05$ using the Shapiro–Wilk (W) statistic for selected daily measurements (each Saturday) and for summed ETo [53]. The normality test indicated that all data were normally distributed. A repeated-measures analysis of variance was conducted to compare estimated total ETo over 27 weeks in 2017 and 2018 for vegetation management treatments. Least significant differences (Duncan's LSD) for the GLM and Tukey's HSD for the GLIMMIX model were used to assess significant differences among treatments in weekly ETo at the 95% probability level. LSD values were calculated using PROC GLM in SAS with an appropriate error term. Two statistical models were constructed to estimate ETo under various vegetative management systems. An Excel spreadsheet was initially developed to solve Equation (1) through a series of steps, utilizing measured meteorological parameters to assess the script's accuracy. Subsequently, a Python-based geographic information system (GIS) script was implemented to calculate ETo using Equation (1) for each vegetation management system. The results from the GIS script were compared with those from the Excel spreadsheet for each treatment to validate the script's accuracy.

3. Results

3.1. Rainfall and Reference Evapotranspiration (ETo) for 2017

In 2017, total annual rainfall measured 878 mm, which is a 5% decrease compared to the 30-year average of 920 mm (Figure 2). The combined rainfall for January, February, and March was 113 mm, approximately 19% below the 30-year average and equivalent to 81% of the 30-year average. In April, rainfall reached 196% of the 30-year average, coinciding with the start of ETo estimation. Rainfall amounts for May, June, July, August, September, and November were 61 mm (50%), 160 mm (170%), 23 mm (23%), 143 mm (167%), 5.59 mm (6%), and 37 mm (43%) of the 30-year average, respectively. October recorded the highest monthly rainfall at approximately 175 mm (216% normal), while December had the lowest at around 3 mm (7.5%). The months with the highest rainfall were April, June, August, and October, each with totals ranging from 145 to 175 mm (Figure 2).

Significant differences ($p < 0.05$) in cumulative ETo were observed among sustainable vegetative management systems from April to October (Table 1). In 2017, the AB, BCa, BCg, and GB management systems exhibited higher ETo compared to the RC treatment (corn crop). The GB treatment recorded the highest ETo at 130 mm, while the corn crop had the lowest at 104 mm. Although no significant differences were observed in the ETo between the BCg (123 mm) and BCa (121 mm) treatments, ETo values were numerically slightly higher for the BCg than the BCa system. The lack of significant differences between BCa and BCg treatments may be attributed to the buffer distance of approximately 35–38 m. Weather sensor locations for both treatments were positioned at the center of the buffer, suggesting that the effects of the tree and grass buffer zones are likely comparable (Table 1). The AB system recorded 115 mm of ETo, a value significantly lower than those observed in the GB and BC (in the agroforestry and grass watersheds) management systems, yet significantly higher than that of the RC treatment.

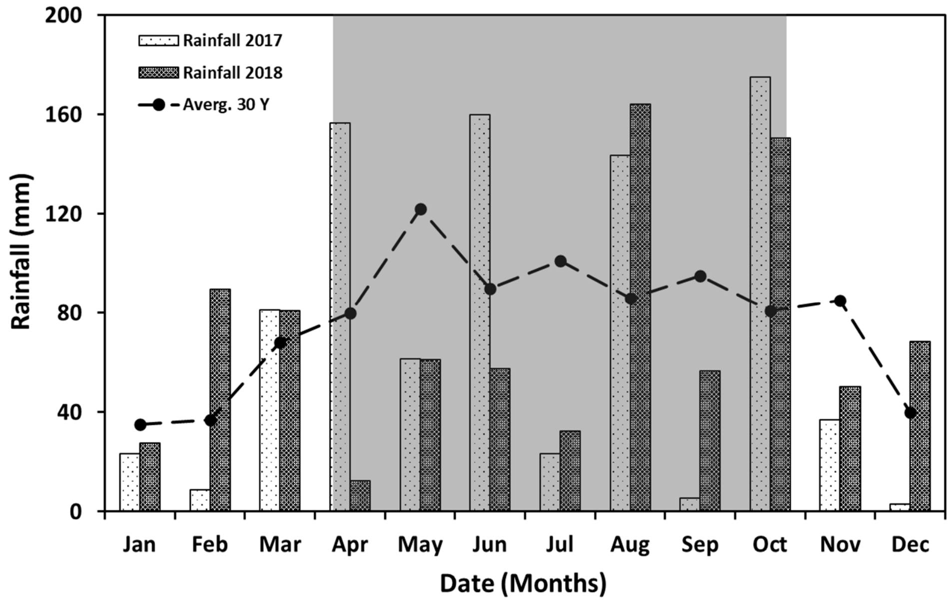

Figure 2. Monthly rainfall distribution for 2017 and 2018 (bars) and 30-year average (long dash) at the University of Missouri Greenley Memorial Research Center in Knox County, Missouri, USA. Shaded areas represent the period of estimated reference evapotranspiration (ETo).

Sustainable management systems significantly affected soil water dynamics during specific weeks of the growing season. For example, during the weeks of 15 April, 6 May, 13 May, 3 June, 10 June, 24 June, 1 July, 8 July, 22 July, and 23 September, these systems exhibited higher estimated daily ETo values, averaging 5.0 to 8.0 mm day^{-1} (Figures 3 and 4). In contrast, the weeks of 29 April, 20 May, 17 June, 15 August, 19 August, 9 September, 23 September, 7 October, and 14 October exhibited the lowest ETo values. These values averaged 1.0 to 4.9 mm day^{-1} (Figures 2–4). These periods coincided with increased precipitation at the study site during these periods, which received 156, 61, 160, 144, and 175 mm of rainfall in April, May, June, August, and September, respectively (Figure 2). Overall, the highest ETo values were observed on 10 June for the GB system, with 8.1 mm day^{-1}, followed by 15 April, with 7.0 mm day^{-1} across all perennial management systems, compared to 2.5 mm day^{-1} for the RC treatment (Figure 3). The lowest ETo values were recorded for the BCg and GB treatments on 29 April (1.0 mm day^{-1}), and for RC management on 29 April, 23 September, and 14 October, with averages from 0.7 to 1.0 mm day^{-1} (Figure 3).

Table 1. The estimated reference evapotranspiration (ETo) (selected Saturday values summed for 27 weeks, April to October) using the Penman–Monteith equation for agroforestry buffer (AB), biofuel crop in agroforestry buffer watershed (BCa), biofuel crop in grass buffer watershed (BCg), grass buffer (GB), and row crop (RC) treatments during 2017 and 2018. Different letters represent significant differences among treatments at $p \leq 0.05$.

Date	2017	2018
Treatment	----------- ETo (mm) -----------	
AB	115 c	105 c
BCa	121 b	108 c
BCg	123 b	112 b
GB	130 a	118 a
RC	104 d	98 d
	Analysis of variation P > F	
Treatment	<0.0001	0.0002

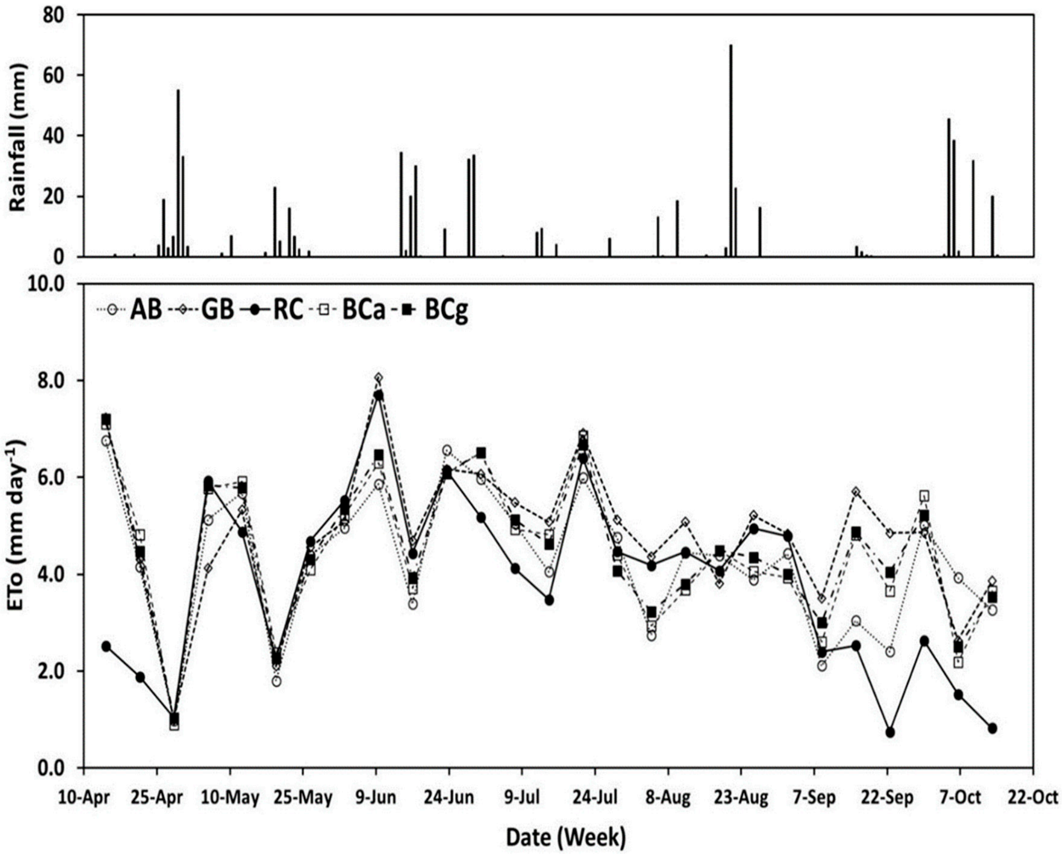

Figure 3. Rainfall distribution (during study period) and effects of vegetation management treatments on reference evapotranspiration (ETo) estimated each Saturday during 2017 (April–October) for agroforestry buffer (AB), biofuel crop in agroforestry buffer watershed (BCa), biofuel crop in grass buffer watershed (BCg), grass buffer (GB), and row crop (corn crop) (RC).

Figure 4 presents the effects of the AB, BCa, BCg, GB, and RC management systems on temporal and spatial ETo, estimated each Saturday from April to October 2017 and visualized using Python-based geographic information systems (GIS). Figure 4 displays raster maps of daily estimated ETo for each Saturday, generated using a Python-based GIS script for all treatments (GB, BCa, BCg, AB, and RC). In these maps, darker areas correspond to higher soil water losses due to ET, while lighter areas indicate lower losses. The results indicate that week's 5, 8, 9, 11, 12 and 15 had the highest estimated ETo values, averaging 5.0–8.0 mm day^{-1} (Figures 3 and 4). Specifically, the average ETo values were 5.0–5.8 mm day^{-1}, 5.0–5.5 mm day^{-1}, 6.0–8.0 mm day^{-1}, 6.1–6.6 mm day^{-1}, 5.2–6.5 mm day $^{-1}$, and 6.0–6.9 mm day^{-1} for weeks 5, 8, 9, 11, 12 and 15, respectively. In contrast, the second-highest ETo values were observed during weeks 7, 10, 13, 14, 16 17, 18, 19, and 20, with ETo ranging from 2.7 to 5.5 mm day^{-1} (Figure 4). The average ETo values for these weeks were 4.1–4.7 mm day^{-1}, 3.4–4.7 mm day^{-1}, 4.1–5.5 mm day^{-1}, 3.5–5.1 mm day^{-1}, 4.1–5.1 mm day^{-1}, 2.7–4.4 mm day^{-1}, 3.7–5.1 mm day^{-1}, 3.8–4.5 mm day^{-1}, and 3.9–5.2 mm day^{-1}, respectively. Week 6 recorded the lowest ETo values, averaging 1.8–2.4 mm day^{-1}, as visualized on the landscape using the Python-based GIS (Figure 4).

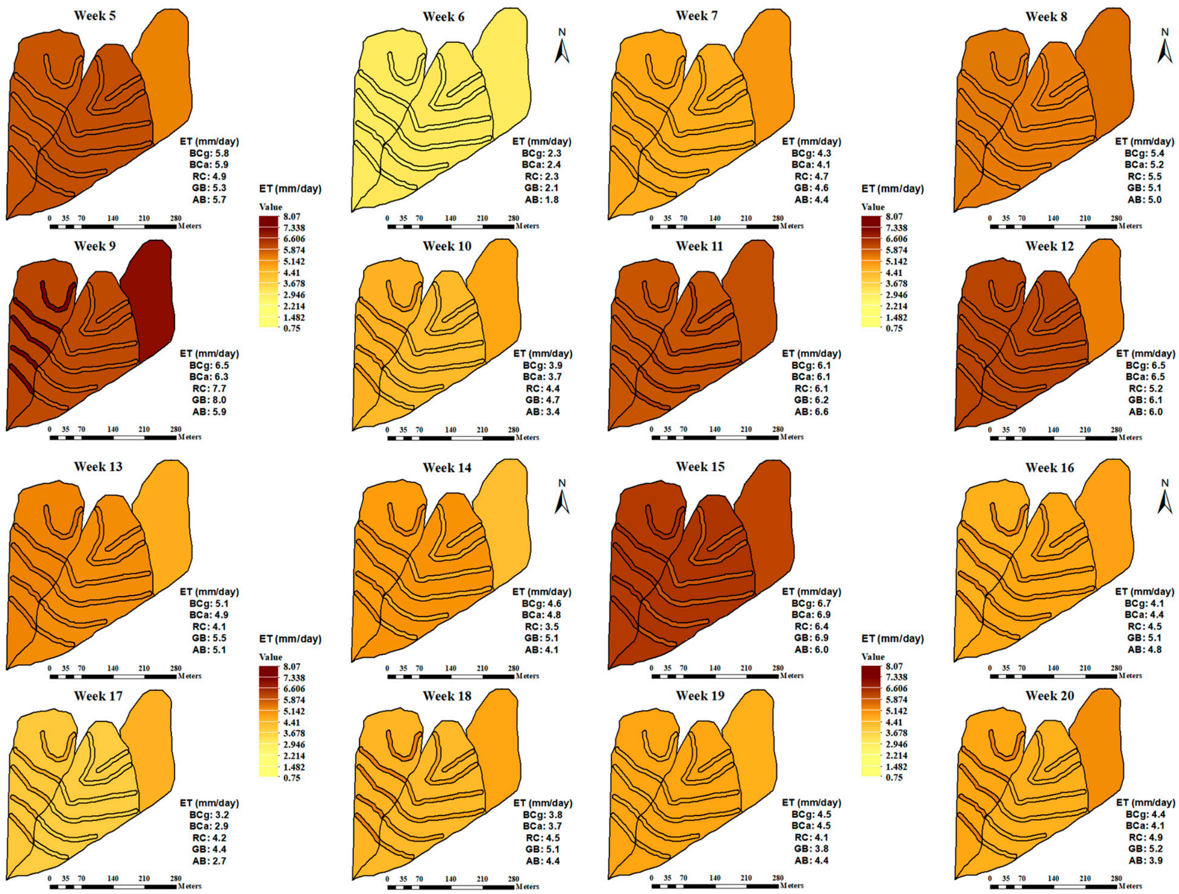

Figure 4. Effects of treatments on temporal and spatial reference evapotranspiration (ETo) estimated each Saturday during 2017 (April–October) and visualized on the landscape using Python-based GIS for agroforestry buffer (AB), biofuel crop in agroforestry buffer watershed (BCa), biofuel crop in grass buffer watershed (BCg), grass buffer (GB), and row crop (corn crop) (RC).

3.2. Rainfall and Reference Evapotranspiration (ETo) for 2018

Figure 2 presents the monthly rainfall data for the study site in 2018. The total annual rainfall was 850 mm, an 8% decrease from the 30-year average of 920 mm. Precipitation during January, February, and March totaled 198 mm, which is 141% of the normal value. April, May, June, and July received 13 mm, 61 mm, 57 mm, and 33 mm, respectively. The highest precipitation was recorded in August and October, with 164 mm (190% of normal) and 150 mm (185% of normal), respectively. In contrast, September and November experienced rainfall below average, at 60% and 59% of the average, respectively. August and October exhibited elevated rainfall, whereas April, May, June, July, and September experienced reduced precipitation. Overall, 2018 was drier than 2017 during the estimated ETo period from April to October.

Table 1 presents the estimated summed ETo values for selected Saturdays over 27 weeks in 2018, while daily values are provided in Figures 5 and 6. In general, Table 1 illustrates that ETo during 2017 was higher than in 2018 for perennial vegetative management systems. The results demonstrate significant differences ($p < 0.05$) among the sustainable vegetative systems. The summed ETo for the AB, BCa, BCg, and GB treatments was 7%, 9%, 14%, and 20% higher, respectively, than for the RC (soybean crop) management (Table 1). The GB treatment recorded the highest summed ETo value at 118 mm, followed by the BCa treatment at 112 mm. While no statistically significant differences were found between the AB and BCa management systems, the BCa treatment exhibited marginally higher numerical values than the AB treatment. The RC treatment had the lowest total ETo among all perennial management systems, at 98 mm. The AB and BCa systems recorded summed ETo values of 105 mm and 108 mm, respectively, which were significantly lower than those observed in the GB and BCg management systems, but significantly higher than that of the RC treatment. Overall, Table 1 shows that the total ETo in 2017 exceeded that of 2018 for perennial vegetative management systems.

Figure 5 presents the rainfall distribution during the study period and illustrates the effects of perennial vegetative treatments on estimated daily ETo for Saturdays over 27 weeks in 2018, as calculated using the Penman–Monteith model. Elevated ETo values were observed on 20 April, 27 April, 15 June, 29 June, 6 July, 27 July, 3 August, and 10 August, corresponding to periods of reduced precipitation, with average values ranging from 4.5 to 7.7 mm day^{-1} (Figures 2, 5 and 6). Conversely, lower ETo values, averaging 0.5 to 4.5 mm day^{-1}, were recorded on 13 April, 4 May, 25 May, 1 June, 8 June, 22 June, 24 August, 31 August, 7 September, 28 September, 5 October, and 12 October (Figures 5 and 6), which coincided with increased rainfall at the study site (Figure 2). The highest ETo values occurred on 20 July for the GB, BCa, and BCg systems, with averages ranging from 7.5 to 7.7 mm day^{-1} (Figure 5). In contrast, the lowest ETo values were estimated on 7 September and 12 October for the GB, BCa, BCg, and RC management systems, with averages between 0.6 and 0.9 mm day^{-1} (Figure 5).

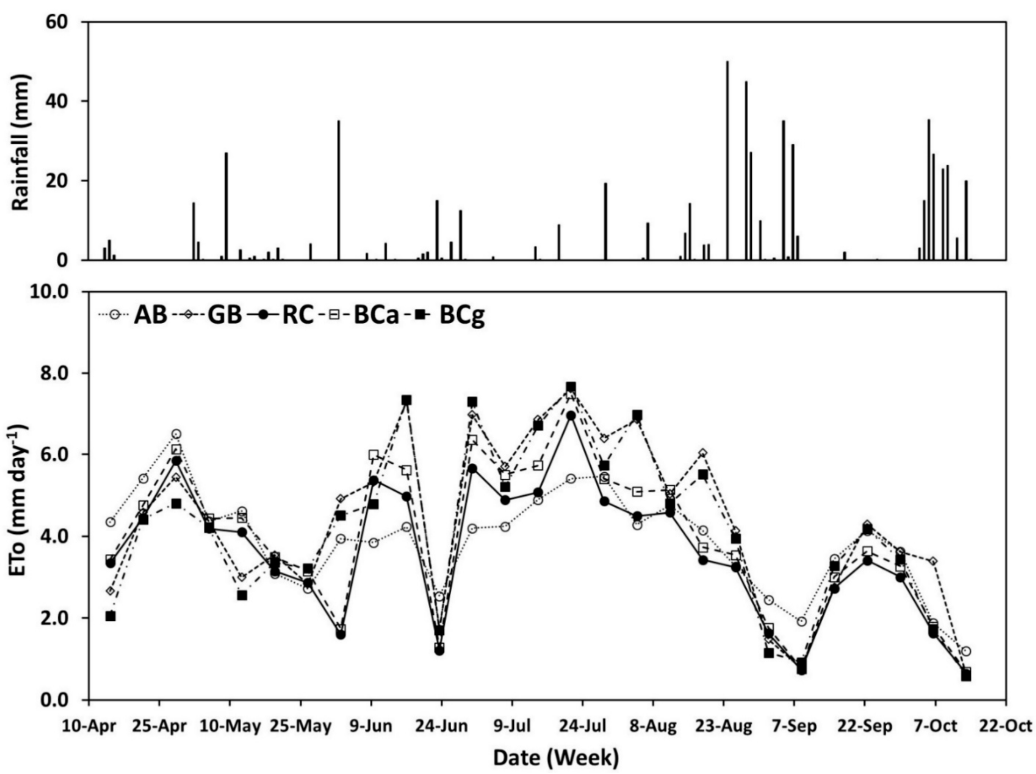

Figure 5. Rainfall distribution (during study period) and effects of vegetation management treatments on reference evapotranspiration (ETo) estimated each Saturday during 2018 (April–October) for agroforestry buffer (AB), biofuel crop in agroforestry buffer watershed (BCa), biofuel crop in grass buffer watershed (BCg), grass buffer (GB), and row crop (corn crop) (RC).

Figure 6 demonstrates the results of daily ETo estimations using the Python-based geographic information system (GIS), collected each Saturday. Figure 4 presents raster maps of daily estimated ETo for each Saturday, generated using the Python-based GIS script for all treatments (GB, BCa, BCg, AB, and RC). Darker areas represent higher soil water losses due to ET, whereas lighter areas indicate lower losses. Previous findings from 2017 indicate that perennial systems exhibit higher water consumption than RC management, attributable to water use and depletion associated with woody and grass perennials throughout the growing season. Figure 6 depicts the effects of the AB, BCa, BCg, GB, and RC systems on temporal and spatial ETo, estimated weekly from April to October 2018 and visualized with the Python-based GIS. The findings showed that week's 9, 10, 12, 13, 14, 15, 16, 17, and 18 had the highest estimated ETo values, with averages ranging from 4.0 to 7.6mm day^{-1} (Figure 6). Particularly, the average ETo values for these weeks were 4.0–6.0 mm day^{-1}, 4.2–7.3 mm day^{-1}, 4.2–7.3 mm day^{-1}, 4.2–5.5 mm day^{-1}, 4.9–6.7 mm day^{-1}, 5.4–7.6 mm day^{-1}, 4.9–6.4 mm day^{-1}, 4.3–7.0 mm day^{-1}, and 4.3–5.1 mm day^{-1}, respectively. In comparison, the second-highest ETo values occurred during weeks 5, 6, 7, 8, 19, and 20, with ETo ranging from 1.6 to 6.0 mm day^{-1} (Figure 6). The average ETo values for these weeks were 2.6–6.6 mm day^{-1}, 3.1–3.5 mm day^{-1}, 2.7–3.2 mm day^{-1}, 1.6–4.5 mm day^{-1}, 3.4–6.0 mm day^{-1}, and 3.2–4.1 mm day^{-1}, respectively. Week 11 exhibited the lowest ETo values, with averages ranging from 1.2 mm day^{-1} in the RC treatment to 2.5 mm day^{-1} in the AB system, as visualized on the landscape using the Python-based GIS (Figure 6).

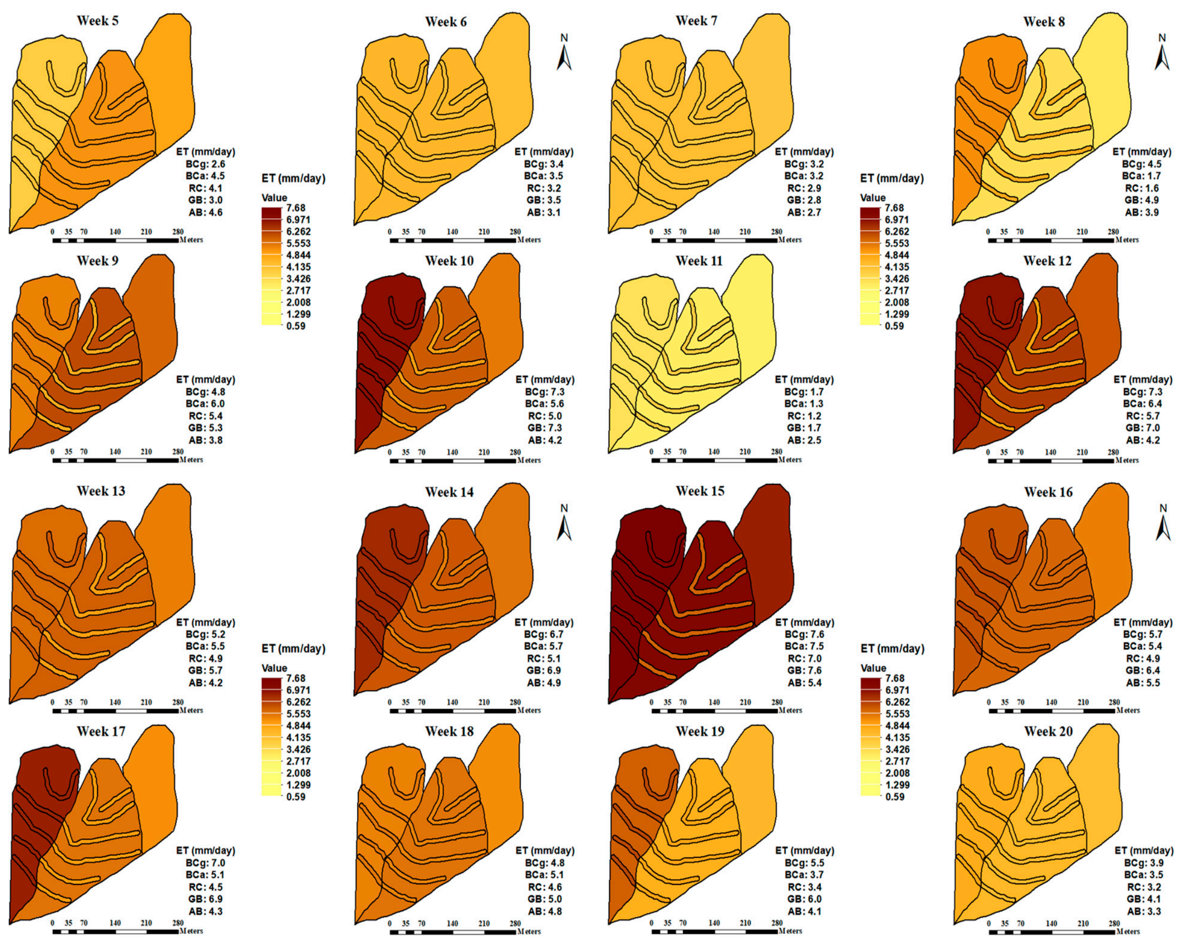

Figure 6. Effects of treatments on temporal and spatial reference evapotranspiration (ETo) estimated each Saturday during 2018 (April–October) and visualized on the landscape using Python-based GIS for agroforestry buffer (AB), biofuel crop in agroforestry buffer watershed (BCa), biofuel crop in grass buffer watershed (BCg), grass buffer (GB), and row crop (corn crop) (RC).

4. Discussion

4.1. Influence of Different Vegetation Systems on Reference Evapotranspiration (ETo) in 2017

Increased rainfall events and enhanced infiltration capacity can result in a larger soil water reservoir in perennial management systems. As a result, greater moisture availability prolongs periods of optimal root-zone wetness, thereby increasing transpiration and reducing surface runoff in degraded claypan landscapes, particularly in the US Midwest [54]. The elevated ETo values observed in perennial vegetative management systems (AB, BC, and GB) relative to the RC treatment from April to July are attributed to increased water use by trees, grass, and switchgrass vegetation systems compared to the RC management (Figure 3). Additionally, increased net radiation in biofuel and grass alleys, resulting from emitted longwave and scattered shortwave radiation from trees, grass, and biofuel management systems over 27 weeks (April to October), may have contributed to higher ETo relative to open areas in the RC management [34,55]. Thus, agroforestry and other perennial management systems offer a significant climate change mitigation strategy by sequestering carbon. Beyond this beneficial biogeochemical impact on global CO_2 concentrations, afforestation influences regional climate by modifying biogeophysical land surface properties [56].

This increase in ETo resulted from greater soil water consumption and reduced rainfall events in 2017 (Figures 2–4). During the post-recharge period, soils managed with perennial vegetative treatments likely exhibited greater profile recharge than those under RC management, due to lower antecedent soil water in the buffer and biofuel treatments prior to the post-recharge interval. As a result, sustainable systems (AB, BC, and GB) showed higher soil water content and greater water storage during these weeks compared to RC [57]. Supporting this finding, previous studies have shown that deeper rooting depths in tree and grass management systems result in greater soil water consumption than in RC management [50,58,59]. Therefore, efficient system design and resource management are essential for achieving economic and environmental sustainability in agroforestry and other perennial systems. Maintaining soil health through effective agricultural management to ensure high infiltration capacity is critical during the rainy season. Furthermore, agroforestry systems can be enhanced by implementing rainwater harvesting for storage and irrigation during the dry season, thereby optimizing soil water resource use [28,35].

Although ET is entirely determined by atmospheric conditions (net radiation, anemometers, humidity, and air temperature), soil organic matter and infiltration affect the response of agroforestry and other perennial systems to ETo and are strongly influenced by site-level soil property changes. Soil organic matter increases ET by enhancing the soil's water-holding capacity, thereby enabling greater water storage [60]. By improving soil structure and increasing the abundance of micro- and macropores, soil organic matter enhances moisture availability for plants, often leading to increased transpiration and, in turn, elevating evaporation from the soil surface [28,36,61]. Thus, perennial vegetative management systems generally promote greater accumulation of organic soil matter [62] and, in turn, exhibit higher proportions of macropores and improved hydraulic properties, including increased saturated hydraulic conductivity [25,28,63]. The favorable soil properties are attributed to increased root exudates and additional organic inputs associated with perennial vegetation management treatments (GB, AB, and BC) over time [25,63]. Such changes in soil properties can reduce surface runoff and increase water-holding capacity and storage, and this effect is particularly notable on claypan landscapes [57]. Agroforestry buffers typically increase ET at the watershed scale by introducing a structural vegetation layer, often composed of deeper-rooted species, into the landscape [36,64]. Although trees reduce soil evaporation by providing shade and lowering surface temperatures, they increase total ET through transpiration by extracting and releasing water from deeper soil layers compared to annual crops [28,36,55]. As agroforestry buffers, they reduce surface runoff by slowing water flow, increasing infiltration, trapping sediment, retaining nutrients, and absorbing excess nutrients to limit groundwater contamination [55].

Several studies [22,57] conducted within the same watersheds evaluated soil water use under sustainable vegetative management practices. These investigations reported higher profile recharge and increased water storage in soils managed with sustainable vegetative systems compared to the RC treatment during recharge periods. Perennial management treatments (AB, BC, and GB) exhibited reduced antecedent soil water during pre-recharge periods due to increased transpiration, leading to enhanced water infiltration and profile recharge following recharge events. Thus, these soil water dynamics are expected to reduce surface runoff, sediment transport, and nutrient losses under perennial vegetative management compared to the RC treatment [31,65]. Collectively, these findings indicate that perennial vegetative management treatments substantially enhance soil water use and ET, thereby improving water infiltration and storage/recharge in the claypan landscapes in the US Midwest [22,57].

The Python script was developed to calculate ETo and visually represent its spatial and temporal variation (Figure 4). The script's accuracy was assessed by comparing its outputs with manual calculations conducted in Excel. The Python script efficiently estimates ETo using the Penman–Monteith model and generates both spatial and temporal visualizations of this parameter. The Python offers greater scalability, automation, and reproducibility than Excel, particularly when managing large or complex datasets [66]. While Excel is suitable for rapid, straightforward calculations and for sharing results with non-technical audiences, the Python is more effective in professional data pipelines and advanced analytics [41,46,66]. Increased ETo under perennial vegetative management systems has been associated with improved water infiltration and reduced surface runoff in degraded soils. The Python script facilitates clear visualization of ET variation across perennial vegetation systems compared to RC management. Previous research [5,50] has demonstrated that employing different ET estimation methods can assist project managers, irrigation engineers, hydrologists, agronomists, and meteorologists in calculating and simulating ET across various vegetation management systems. Therefore, accurate evaluation of ETo is critical for effective land management in agricultural and wetland restoration settings, as it determines atmospheric water demand, supports precise crop irrigation, and sustains hydrological balance in restored ecosystems [46]. The ET demonstrates both spatial and temporal variability, shaped by vegetation, soil properties, and climatic factors throughout the year [33]. These dynamics underscore the significant influence of land–atmosphere interactions on local drought conditions. The Python-based GIS script simulates the ET component of the water balance by estimating actual/reference ET using meteorological inputs, soil moisture, and land cover data. This methodology enables comprehensive landscape analysis and integration with other hydrological cycle components, thereby supporting the evaluation of landscape vulnerability to climate change [41].

Perennial systems enhance water management by utilizing deep root systems and continuous canopy cover to increase ET, thereby reducing soil moisture during pre-replenishment periods [28,57,67]. This process improves the soil's capacity to absorb rainfall, decreases surface runoff, and provides a sustainable buffer against flooding and erosion [22,31]. Leveraging the spatial variability of ET allows for the strategic placement of buffer zones, such as riparian forests, to optimize water balance management by aligning ET losses with soil moisture retention and groundwater recharge requirements [28]. Climate extremes, including prolonged droughts and intense rainfall events, are

https://doi.org/10.3390/su18105209

generally projected to intensify, posing significant threats to the global water cycle and agricultural productivity [68]. Thus, estimating ET is essential in climate studies, serving as a key indicator of agricultural water stress and contributing to atmospheric moisture that intensifies climate extremes, underscoring the need for precise ET monitoring for adaptive agricultural management and drought mitigation [68].

4.2. Influence of Different Vegetation Systems on Reference Evapotranspiration (ETo) in 2018

Table 1 shows that the summed ETo in 2017 was higher than in 2018 for perennial vegetative management systems. This difference is attributed to greater rainfall in 2017 (668 mm) compared to 2018 (580 mm) during the ETo estimation period. Moreover, the 2017 corn crop consumed more water than the 2018 soybean crop. These findings are consistent with Copeland et al. [69], who reported that corn depletes water more than soybeans, primarily due to its determinate growth cycle and substantially higher leaf area index, which leads to increased ET during peak summer months. Furthermore, this variation in water content during pre- and post-recharge periods for buffer and biofuel management systems can be attributed to higher root density and increased root decay at the soil surface [22]. In addition, perennial management practices improve soil structure by promoting deeper root systems, thereby increasing the proportion of macropores and reducing surface runoff and soil and nutrient losses [25,28]. Lastly, these sustainable vegetative systems are more effective at storing organic soil matter than continuous monoculture systems [27,63], due to greater root biomass and less disturbance.

To support the findings in Figures 5 and 6, Alagele et al. [57] conducted the study in the same watersheds and reported that three principal recharge periods occurred after soil water depletion in 2017, whereas two occurred in 2018. In both years, soil water content was lower for the AB, BC, and GB management treatments than for the RC treatment prior to the recharge period. After the recharge periods, soil water content in the AB, GB, and BC treatments increased more than in the RC treatment. These observed differences in soil water content in perennial management systems, relative to the RC management, were likely attributable to greater soil water consumption through transpiration by trees and grasses during the pre-recharge period and enhanced infiltration during the post-recharge period [18,22]. In agreement with our study, the study conducted by [70] found that the agroforestry system maintained significantly higher soil moisture compared to RC management. This significantly higher soil moisture content during the dry spell compared to conventional winter wheat was caused by the high soil organic matter content and low bulk density in agroforestry tree systems, which contributed to conserve soil moisture [70]. Also, this study demonstrated that agroforestry systems can buffer soil moisture availability to tolerate the drought conditions in agroforestry systems compared to conventional winter wheat [70]. This finding can be attributed to the microclimate environment due to several factors like reduced evaporation, increased soil organic matter, and higher plant diversity in the agroforestry system compared to conventional crop production systems [64]. Extensive root systems and increased rooting depth in perennial systems significantly increase ET by improving water access, particularly during dry periods [71]. These roots modify soil physical structure, thereby enhancing hydraulic conductivity and water infiltration [28,63]. Consequently, plants with deep root systems can access soil moisture reservoirs that are inaccessible to shallow-rooted species. This adaptation enables survival during severe droughts, supports active transpiration in dry seasons, and promotes long-term stability in arid ecosystems [22]. Perennial management practices enable more efficient resource use than a monocropping system, as the structural and functional diversity within mixed-cropping canopies supports sustained greenness, improved drought resilience, and greater seasonal biomass production [72].

To provide context for the data analysis, Figure 6 presents the findings of daily ETo, conducted each Saturday using the Python-based GIS. As previously discussed, perennial systems require greater water consumption than RC management due to the water use and depletion associated with woody and grass perennial management practices throughout the growing season [57]. As a result, these systems retain greater amounts of water after infiltration events, which provides a more stable moisture supply for vegetation during prolonged dry periods [12,22]. To ensure the accuracy of these results, the Python-based GIS script was validated by comparing its calculations with those obtained from an Excel spreadsheet. Notably, the ETo estimates generated by the Python script for 2017 and 2018 were identical to those produced in Excel, with the Python script providing results within seconds, whereas Excel required several hours. This finding underscores Python scripts' greater efficiency in ETo calculations, as they yield results equivalent to those produced by Excel but complete computations within seconds rather than hours [40,46,66,73]. This advantage arises from the Python's optimized processing of large-scale tabular data and its capacity for automated workflows, while Excel frequently encounters limitations during complex, iterative operations [73]. Furthermore, both methods produced consistent ETo values for 2017 and 2018 using the Penman–Monteith model. Together, these results demonstrate that a GIS-based Python script can be effectively utilized to generate raster maps for simulating and visualizing ET across diverse landscapes and management systems [40,46]. Thus, the application of Python within ArcGIS in this simulation facilitates assessment of the impact of development on the water cycle and future water availability, and this approach allows planners to optimize stormwater management and evaluate various land-use scenarios [41].

The key findings of this study are that perennial vegetative systems reduce surface runoff and nutrient loss by increasing ET and water consumption, as they consume more water during pre-recharge periods and retain more soil water following post-infiltration events. These effects are particularly significant in wet regions, such as the Putnam and Kilwinning soils of the U.S. Midwest (mean annual precipitation of 920 mm), which possess a drainage-restrictive B horizon [22,57]. Conversely, in dry regions, the main limitation of perennial vegetation systems is their greater water use and susceptibility to hydraulic failure during prolonged droughts, which can result in lower yields than those of annual crops in water-limited environments [69,71]. While perennial systems contribute to soil conservation, their extensive root systems may deplete soil moisture reserves more quickly than they are replenished in aridic soil moisture regimes [28,74]. Therefore, selecting saline- and drought-resistant crop and tree varieties is a critical strategy for sustainable agriculture in dry regions [75]. This strategy is vital for ensuring food security, reclaiming degraded land, and adapting to climate change [24,28,29]. Sustainable management practices should be tailored for the availability of local water resources to ensure that consumption rates do not exceed natural replenishment, thereby sustaining long-term water security. Thus, crop and tree selection should utilize a multi-criteria approach that prioritizes water availability, soil characteristics, and climate factors to effectively manage ET and promote sustainable productivity [3,35,38,68,71,75]. Appropriate selection should account for the fact that elevated evaporation rates, especially in hot climates, substantially increase water requirements [66,71]. Interestingly, the ET spatial distribution map offers a valuable decision-support tool for determining buffer zone spacing and selecting appropriate tree species.

5. Conclusions

A long-term paired watershed study conducted in the claypan region of Northeast Missouri evaluated the effects of perennial systems on ETo, estimated using the Penman–Monteith equation, in comparison to the RC treatment during 2017 and 2018. The findings

https://doi.org/10.3390/su18105209

demonstrate that perennial systems enhance water regulation by modulating ETo dynamics, a fundamental aspect of sustainable land management, because ET is a critical process linking vegetation management, water balance, and land sustainability. Perennial systems exhibited higher ETo and greater soil water consumption than RC management in both years. In 2017, both perennial and RC systems recorded higher ETo than in 2018, likely due to increased precipitation. Thus, in areas with higher water availability, increasing ET by establishing perennial buffer zones during the pre-replenishment period can lower soil moisture, thereby reducing rainy-season runoff and nutrient loss. The ETo spatial distribution map generated using Python GIS enables the identification of water consumption hotspots within the watershed and supports the optimization of buffer zone spacing and tree species selection. At the policy level, integrating ET indicators into agricultural environmental performance evaluation systems is recommended.

This study presents a novel methodology for estimating ET across a range of vegetative management systems. The results offer actionable insights for farmers and policymakers regarding water-use differences among management systems on degraded soils and inform the design of perennial multispecies systems that minimize losses of water. Understanding ET variability is essential for developing effective land management strategies. The Python-based geographic information system (GIS) developed in this study provides a robust tool for estimating and visualizing ET across heterogeneous landscapes and management systems, and ETo estimates were consistent between the Python-based GIS script and Excel calculations. While this study offers valuable insights for future research and practical agricultural applications in this region, subsequent investigations should address a broader range of soil types, climatic conditions, and vegetative management systems to estimate ET using the Python-based geographic information system (GIS). Importantly, it should be noted that the conclusions drawn from this study are applicable to this site and do not extend beyond the data.

Author Contributions: Conceptualization, S.M.A., S.H.A. and R.P.U.; Methodology, S.M.A., S.H.A. and R.P.U.; Software, S.M.A.; Validation, S.M.A., S.H.A. and R.P.U.; Formal analysis, S.M.A., S.H.A. and R.P.U.; Investigation, S.M.A., S.H.A. and R.P.U.; Resources, S.M.A., S.H.A. and R.P.U.; Data curation, S.M.A., S.H.A. and R.P.U.; Writing-original draft, S.M.A.; Writing-review & editing, S.M.A., S.H.A. and R.P.U.; Visualization, S.M.A.; Supervision, S.M.A., S.H.A. and R.P.U.; Project administration, S.M.A.; Funding acquisition, S.M.A., S.H.A. and R.P.U. All authors have read and agreed to the published version of the manuscript.

Funding: This study was funded through the University of Missouri–Columbia/Center for Agroforestry under cooperative agreement 58-6020-6-001 with the USDA-ARS, as well as the Iraqi Ministry of Higher Education and Scientific Research.

Institutional Review Board Statement: Not applicable.

Informed Consent Statement: Not applicable.

Data Availability Statement: The data supporting this study will be made available upon reasonable request to the corresponding author.

Acknowledgments: The University of Missouri–Columbia/Center for Agroforestry and the Iraqi Ministry of Higher Education and Scientific Research are acknowledged for their contributions to support this study. Additionally, we would like to thank Kelly Nelson and all the individuals at the University of Missouri/Greenley Research Center in Novelty, Missouri, USA, for their field assistance.

Conflicts of Interest: The authors declare no conflicts of interest.

Abbreviations

AB, agroforestry buffer; BC, biofuel crop; BCa, biofuel crop in the agroforestry watershed; BCg, biofuel crop in the grass watershed; GB, grass buffer; ETo, reference evapotranspiration; GIS, geographic information system; RC, row crop.

References

1. Pereira, A.; Pires, L. Evapotranspiration and water management for crop production. In *Evapotranspiration—From Measurements to Agricultural and Environmental Applications*; Gerosa, G., Ed.; InTech Publishing: Rijeka, Croatia, 2011; pp. 143–166.
2. Ezenne, G.I.; Eyibio, N.U.; Tanner, J.L.; Asoiro, F.U.; Obalum, S.E. An overview of uncertainties in evapotranspiration estimation techniques. *J. Agrometeorol*. **2023**, *25*, 173–182. https://doi.org/10.54386/jam.v25i1.2014.
3. Rua, M.L.; Fernandes, G.S.T.; Franco, T.M.; Santos, M.G.M.; Nery, M.K.M.; Vasconcelos, A.J.S.; Navarro, L.M.; Dias, J.S.; Conceição, J.B.; Oliveira, I.A.; et al. Evapotranspiration and Crop Coefficient of Economically Important Fruit Trees in the Eastern Amazon. *J. Hydrol.* **2026**, *13*, 108. https://doi.org/10.3390/hydrology13040108.
4. Yang, Y.; Roderick, M.L.; Guo, H.; Miralles, D.G.; Zhang, L.; Fatichi, S.; Luo, X.; Zhang, Y.; McVicar, T.R.; Tu, Z.; et al. Evapotranspiration on a greening Earth. *Nat. Rev. Earth Environ*. **2023**, *9*, 626–641. https://doi.org/10.1038/s43017-023-00464-3.
5. Priyadharshini, S.; Canessane, R.A. Evaluation of evapotranspiration for agricultural crops. In *2015 IEEE International Conference on Computational Intelligence and Computing Research* (ICCIC); IEEE: New York, NY, USA, 2015, pp. 1–5. https://doi.org/10.1109/ICCIC.2015.7435702.
6. Shadmehri Toosi, A.; Batelaan, O.; Shanafield, M.; Guan, H. Land use-land cover and hydrological modeling: A review. *Water* **2025**, *12*, e70013. https://doi.org/10.1002/wat2.70013.
7. Cai, X.; Zhang, X.; Noël, P.H.; Shafiee-Jood, M. Impacts of climate change on agricultural water management: A review. *Water* **2015**, *2*, 439–455. https://doi.org/10.1002/wat2.1089.
8. Eshete, D.G.; Sinshaw, B.G.; Legese, K.G. Critical review on improving irrigation water use efficiency: Advances, challenges, and opportunities in the Ethiopia context. *Water-Energy Nexus* **2020**, *3*, 143–154. https://doi.org/10.1016/j.wen.2020.09.001.
9. Yang, X.; Shi, X.; Zhang, Y.; Tian, F.; Ortega-Farias, S. Response of evapotranspiration (ET) to climate factors and crop planting structures in the Shiyang River Basin, Northwestern China. *Remote Sens*. **2023**, *15*, 3923. https://doi.org/10.3390/RS15163923.
10. Eslamian, S.; Khordadi, M.J.; Abedi-Koupai, J. Effects of variations in climatic parameters on evapotranspiration in the arid and semi-arid regions. *Glob. Planet. Change* **2011**, *78*, 188–194. https://doi.org/10.1016/j.gloplacha.2011.07.001.
11. Subedi, A.; Chávez, J.L. Crop evapotranspiration (ET) estimation models: A review and discussion of the applicability and limitations of ET methods. *J. Agric. Sci*. **2015**, *7*, 50–68. https://doi.org/10.5539/jas.v7n6p50.
12. Djaman, K.; Irmak, S. Soil water extraction patterns and crop, irrigation, and evapotranspiration water use efficiency of maize under full and limited irrigation and rainfed settings. *Trans. ASABE* **2012**, *55*, 1223–1238. https://doi.org/10.13031/2013.42262.
13. Abada, Y.; El Beqqali, O.; Riffi, J.; El Idrissi, M.; Bouramtane, T. Daily reference evapotranspiration estimation using sequential and ensemble learning approaches: A case study in a high-evaporation region. *J. Hydrol. Reg. Stud*. **2026**, *65*, 103454. https://doi.org/10.1016/j.ejrh.2026.103454.
14. Wanniarachchi, S.; Sarukkalige, R. A review on evapotranspiration estimation in agricultural water management: Past, present, and future. *J. Hydrol*. **2022**, *9*, 123. https://doi.org/10.3390/hydrology9070123.
15. Wallace, J.S. Increasing agricultural water use efficiency to meet future food production. *Agric. Ecosyst. Environ*. **2000**, *82*, 105–119. https://doi.org/10.1016/S0167-8809(00)00220-6.
16. Evans, R.G.; Sadler, E.J. Methods and technologies to improve efficiency of water use. *Water Resour. Res*. **2008**, *44*, 1–15. https://doi.org/10.1029/2007WR006200.
17. Kumar, R.; Shambhavi, S.; Kumar, R.; Singh, Y.K.; Rawat, K.S. Evapotranspiration mapping for agricultural water management: An overview. *J. Appl. Nat. Sci.* **2013**, *5*, 522. https://doi.org/10.31018/jans.v5i2.363.
18. Koech, R.; Langat, P. Improving irrigation water use efficiency: A review of advances, challenges and opportunities in the Australian context. *Water* **2018**, *10*, 1771. https://doi.org/10.3390/w10121771.
19. Blatchford, M.L.; Mannaerts, C.M.; Zeng, Y.; Nouri, H.; Karimi, P. Status of accuracy in remotely sensed and in-situ agricultural water productivity estimates: A review. *Remote Sens. Environ*. **2019**, *234*, 111413. https://doi.org/10.1016/j.rse.2019.111413.
20. Mavridou, E.; Vrochidou, E.; Papakostas, G.A.; Pachidis, T.; Kaburlasos, V.G. Machine Vision Systems in Precision Agriculture for Crop Farming. *J. Imaging* **2019**, *5*, 89. https://doi.org/10.3390/jimaging5120089.

21. Abdelhak, M. Innovative Techniques for Soil and Water Conservation. In *Ecosystem Management: Climate Change and Sustainability*, 1st Ed.; Banerjee, A., Jhariya, M.K., Raj, A., Mechergui, T., Eds.; John Wiley & Sons: Austin, TX, USA, 2024; pp. 291–326.
22. Anderson, S.H.; Udawatta, R.P.; Seobi, T.; Garrett, H.E. Soil water content and infiltration in agroforestry buffer strips. *Agrofor. Syst.* **2009**, *75*, 5–16. https://doi.org/10.1007/s10457-008-9128-3.
23. Schmitt, T.; Dosskey, M.G.; Hoagland, K.D. Filter strip performance and processes for different vegetation, widths, and contaminants. *J. Environ. Qual*. **1999**, *28*, 1479–1489. https://doi.org/10.2134/jeq1999.00472425002800050013x.
24. Lal, R. Restoring soil quality to mitigate soil degradation. *Sustainability* **2015**, *7*, 5875–5895. https://doi.org/10.3390/su7055875.
25. Alagele, S.M.; Anderson, S.H.; Udawatta, R.P.; Veum, K.S.; Rankoth, L.M. Effects of conservation practices on soil quality compared with a corn-soybean rotation on a claypan soil. *J. Environ. Qual*. **2019**, *48*, 1694–1702. https://doi.org/10.2134/jeq2019.03.0121.
26. Han, Y.; Feng, G.; Ouyang, Y. Effects of soil and water conservation practices on runoff, sediment and nutrient losses. *Water* **2018**, *10*, 1–13. https://doi.org/10.3390/w10101333.
27. Zaibon, S.; Anderson, S.H.; Kitchen, N.R.; Haruna, S.I. Hydraulic properties affected by topsoil thickness in switchgrass and corn-soybean cropping systems. *Soil Sci. Soc. Am. J.* **2016**, *80*, 1365–1376. https://doi.org/10.2136/sssaj2016.04.0111.
28. Alagele, S.M.; Anderson, S.H.; Udawatta, R.P. Conservation buffers and soil water. In *Soil Hydrology in a Changing Climate*, 1st ed.; Blanco, H., Kumar, S., Anderson, S.H., Eds.; CSIRO Publishing: Clayton, Australia, 2022; pp. 133–156.
29. Verchot, L.V.; Van Noordwijk, M.; Kandji, S.; Tomich, T.; On, C.; Albrecht, A.; Mackensen, J.; Bantilan, C.; Anupama, K.V.; Palm, C. Climate change: Linking adaptation and mitigation through agroforestry. *Mitig. Adapt. Strat. Gl*. **2007**, *12*, 901–918. https://doi.org/10.1007/s11027-007-9105-6.
30. Ong, C.K.; Wilson, J.; Deans, J.D.; Mulayta, J.; Raussen, T.; Wajja-Musukwe, N. Tree–crop interactions: manipulation of water use and root function. *Agric. Water Manag*. **2002**, 53, 171-186. https://doi.org/10.1016/S0378-3774(01)00163-9.
31. Udawatta, R.P.; Krstansky, J.J.; Henderson, G.S.; Garrett, H.E. Agroforestry practices, runoff, and nutrient loss. *J. Environ. Qual*. **2002**, *31*, 1214–1225. https://doi.org/10.2134/jeq2002.1214.
32. Breil, M.; Krawczyk, F.; Pinto, J. The response of the regional longwave radiation balance and climate system in Europe to an idealized afforestation experiment. *Earth Syst. Dyn. Discuss*. **2022**, *14*, 243–253. https://doi.org/10.5194/esd-14-243-2023.
33. Rodriguez-Iturbe, I.; D'odorico, P.; Porporato, A.; Ridolfi, L. On the spatial and temporal links between vegetation, climate, and soil moisture. *Water Resour. Res*. **1999**, *35*, 3709–3722. https://doi.org/10.1029/1999WR900255.
34. Svoma, B.M.; Fox, N.I.; Pallardy, Q.; Udawatta, R.P. Evapotranspiration differences between agroforestry and grass buffer systems. *Agric. Water Manag*. **2016**, *176*, 214–221. https://doi.org/10.1016/j.agwat.2016.06.018.
35. Pham, H.T.; Barron, J.; Bergkvist, G.; Öborn, I.; La, N.; Mulia, R.; Dahlin, A.S. Tree rows and grass-strips increase water availability in fruit tree-crop agroforestry systems on sloping land. *J. Agric. Food Res*. **2025**, *22*, 102045. https://doi.org/10.1016/j.jafr.2025.102045.
36. Jose, S. Agroforestry for ecosystem services and environmental benefits: An overview. *Agrofor. Syst*. **2009**, *76*, 1–10. https://doi.org/10.1007/s10457-009-9229-7.
37. Pandey, A.; Tiwari, P.; Manpoong, C.; Jatav, H.S. Agroforestry for restoring and improving soil health. In *Agroforestry to Combat Global Challenges: Current Prospects and Future Challenges*; Springer Nature: Singapore, 2024; pp. 147–164.
38. Sutterlütti, R.; Kayser, M.; Komainda, M.; Isselstein, J. Alley cropping tree lines alter temperature and light quantity and influence daily growth rates of grassland. *Grass Forage Sci*. **2023**, *78*, 402–415. https://doi.org/10.1111/gfs.12618.
39. Taheri, M.; Bigdeli, M.; Imanian, H.; Mohammadian, A. An overview of evapotranspiration estimation models utilizing artificial intelligence. *Water* **2025**, *17*, 1384. https://doi.org/10.3390/w17091384.
40. Mohammed, M.G.; Trauth, K.M. GIS-Based Python Simulation of Infiltration over a Landscape. *J. Irrig. Drain. Eng*. **2020**, *146*, 06020008. https://doi.org/10.1061/(ASCE)IR.1943-4774.0001495.
41. Wang, Z.; Trauth, K.M. Development of GIS-based Python scripts to calculate a water surface profile on a landscape for wetlands decision-making. *J. Hydroinform*. **2020**, *22*, 628–640. https://doi.org/10.2166/hydro.2020.167.
42. Zandbergen, P.A. *Python Scripting for ArcGIS*; Esri Press: Redlands, CA, USA, 2015.
43. Toms, S.; Parker, B.; Tucker, C.; Rubalcava, R. *Python for ArcGIS Pro: Automate Cartography and Data Analysis Using ArcPy, ArcGIS API for Python, Notebooks, and Pandas*; Packt Publishing Ltd.: Birmingham, UK, 2022.
44. Hernán Jimenez-Palomino, W.; Miguel Soto-Juscamayta, L.; Henrry Catamayo-Barrios, J.; Leonardo Bendezú-Prado, J.; Berrocal-Argumedo, K.; Agustín Esparta-Sanchez, J.; Margarita Maldonado-Lacua, G.; Cesar Mayorga-Rojas, J.; Alberto

Romero-Baylon, A. Implementation of a GIS for the Conservation of Irrigation Canals: Using ArcGIS and Python for Automation. *Math. Model. Eng. Probl*. **2024**, *11*, 2337–2346. https://doi.org/10.18280/mmep.110907.
45. Lacayo, M.; Rodila, D.; Giuliani, G.; Lehmann, A. A framework for ecosystem service assessment using GIS interoperability standards. *Comput. Geosci*. **2021**, *154*, 104821. https://doi.org/10.1016/j.cageo.2021.104821.
46. Mohammed, M.G.; Trauth, K.M. A Python-based GIS simulation of the spatial and temporal variation in evapotranspiration. *Appl. Eng. Agric*. **2019**, *35*, 759–765. https://doi.org/10.13031/aea.13139.
47. Nasrollahpour, R.; Skorobogatov, A.; He, J.; Valeo, C.; Chu, A.; Van Duin, B. The impact of vegetation and media on evapotranspiration in bioretention systems. *Urban For. Urban Green*. **2022**, *74*, 127680. https://doi.org/10.1016/j.ufug.2022.127680.
48. Owenby, J.; Ezell, D. *Climatography of the United States No. 81—Monthly Station Normals of Temperature, Precipitation, and Heating and Cooling Degree Days, 1961–1990*; National Oceanic and Atmospheric Administration National Climatic Data Center: Asheville, NC, USA, 1992.
49. Veum, K.S.; Goyne, K.W.; Holan, S.H.; Motavalli, P.P. Assessment of soil organic carbon and total nitrogen under conservation management practices in the Central Claypan Region, Missouri, USA. *Geoderma* **2011**, *167*, 188–196. https://doi.org/10.1016/j.geoderma.2011.09.003.
50. Allen, R.G.; Pereira, L.S.; Raes, D.; Smith, M. Crop evapotranspiration: Guidelines for computing crop water requirements. In *FAO Irrigation and Drainage Paper No 56*; Food and Agriculture Organization Land and Water: Rome, Italy, 1998; pp 174.
51. Zotarelli, L.; Dukes, M.D.; Romero, C.C.; Migliaccio, K.W.; Morgan, K.T. *Step by Step Calculation of the Penman-Monteith Evapotranspiration (FAO-56 Method)*; EDIS: Gainesville, FL, USA, 2020.
52. Institute, S.A.S. SAS User's Guide. In *Statistics*; SAS Inst: Cary, NC, USA, 2013.
53. Shapiro, S.S.; Wilk, M.B. An analysis of variance test for normality (complete samples). *Biometrika* **1965**, *52*, 591–611.
54. Hess, L.J.; Hinckley, E.L.S.; Robertson, G.P.; Hamilton, S.K.; Matson, P.A. Rainfall intensification enhances deep percolation and soil water content in tilled and no-till cropping systems of the US Midwest. *Vadose Zone J.* **2018**, *17*, 1–12. https://doi.org/10.2136/vzj2018.07.0128.
55. Brandle, J.R.; Hodges, L.; Zhou, X.H. Windbreaks in North American agricultural systems. *Agrofor. Syst*. **2004**, *61*, 65–78. https://doi.org/10.1023/B:AGFO.0000028990.31801.62.
56. Wang, Y.; Yan, X.; Wang, Z. The biogeophysical effects of extreme afforestation in modeling future climate. *Theor. Appl. Climatol.* **2014**, *118*, 511-521. https://doi.org/10.1007/s00704-013-1085-8.
57. Alagele, S.M.; Anderson, S.H.; Udawatta, R.P. Agroforestry, grass, biofuel crop, and row-crop management effects on soil water dynamics for claypan landscapes. *Soil Sci. Soc. Am. J.* **2020**, *84*, 203–219. https://doi.org/10.1002/saj2.20026.
58. Seyfried, M.S.; Wilcox, B.P. Soil water storage and rooting depth: key factors controlling recharge on rangelands. *Hydrol. Process*. **2006**, *20*, 3261-3275. https://doi.org/10.1002/hyp.6331.
59. Schenk, H.J.; Jackson, R.B. Rooting depths, lateral root spreads and below-ground/above-ground allometries of plants in water-limited ecosystems. *J. Ecol*. **2002**, *90*, 480–494. https://doi.org/10.1046/j.1365-2745.2002.00682.x.
60. Feifel, M.; Durner, W.; Hohenbrink, T.L.; Peters, A. Effects of improved water retention by increased soil organic matter on the water balance of arable soils: A numerical analysis. *Vadose Zone J*. **2024**, *23*, e20302. https://doi.org/10.1002/vzj2.20302.
61. Ankenbauer, K.J.; Loheide, S.P. The effects of soil organic matter on soil water retention and plant water use in a meadow of the Sierra Nevada, CA. *Hydrol. Process*. **2017**, *31*, 891–901. https://doi.org/10.1002/hyp.11070.
62. Kumar, S.; Anderson, S.H.; Udawatta, R.P.; Kallenbach, R.L. Water infiltration influenced by agroforestry and grass buffers for a grazed pasture system. *Agrofor. Syst*. **2012**, *84*, 325–335. https://doi.org/10.1007/s10457-011-9474-4.
63. Seobi, T.; Anderson, S.H.; Udawatta, R.P.; Gantzer, C.J. Influence of grass and agroforestry buffer strips on soil hydraulic properties for an Albaqualf. *Soil Sci. Soc. Am. J*. **2005**, *69*, 893–901. https://doi.org/10.2136/sssaj2004.0280.
64. Fahad, S.; Chavan, S.B.; Chichaghare, A.R.; Uthappa, A.R.; Kumar, M.; Kakade, V.; Pradhan, A.; Jinger, D.; Rawale, G.; Poczai, P. Agroforestry systems for soil health improvement and maintenance. *Sustainability* **2022**, *14*, 14877. https://doi.org/10.3390/su142214877.
65. Weerasekara, C.; Udawatta, R.P.; Jose, S.; Kremer, R.J.; Weerasekara, C. Soil quality differences in a row-crop watershed with agroforestry and grass buffers. *Agrofor. Syst*. **2016**, *90*, 829–838. https://doi.org/10.1007/s10457-016-9903-5.
66. Ali, O.M.; Breik, M.; Aly, T.; Raslan, A.D.; Gheith, M. Enhancing Data Analysis and Automation: Integrating Python with Microsoft Excel for Non-Programmers. *J. Softw. Eng. Appl*. **2024**, *17*, 530–540. https://doi.org/10.4236/jsea.2024.176030.
67. Kokila, A.; Nagarajaiah, C.; Hanumanthappa, D.C.; Shivanna, B.; Sathish, K.; Mahadevamurthy, M. Effect of tree canopy cover on soil moisture dynamics in different agroforestry systems under semi-arid condition. *Int. J. Environ. Clim. Change* **2024**, *14*, 485–495. https://doi.org/10.9734/ijecc/2024/v14i94432.

68. Disasa, K.N.; Yan, H.; Zhang, J.; Wang, G.; Zhang, C.; Zhang, D.; Wang, B.; Hao, B. Comprehensive review of drought characteristics and intensification under climate change: Implications for agriculture and water resources. *J. Hydrol.* **2025**, *664*, 134571. https://doi.org/10.1016/j.jhydrol.2025.134571.
69. Copeland, P.J.; Allmaras, R.R.; Crookston, R.K.; Nelson, W.W. Corn-soybean rotation effects on soil water depletion. *J. Agron*. **1993**, *85*, 203–210. https://doi.org/10.2134/agronj1993.00021962008500020008x.
70. Chaudhary, V.P.; Ghaley, B.B. Insights into beneficial effects of an agroforestry system on soil properties and crop yields: A case study from the experimental farm at University of Copenhagen, Denmark. *Sustainability* **2025**, *17*, 1466. https://doi.org/10.3390/su17041466.
71. Kühnhammer, K.; Van Haren, J.; Kübert, A.; Bailey, K.; Dubbert, M.; Hu, J.; Ladd, S.N.; Meredith, L.K.; Werner, C.; Beyer, M. Deep roots mitigate drought impacts on tropical trees despite limited quantitative contribution to transpiration. *Sci. Total Environ*. **2023**, *893*, 164763. https://doi.org/10.1016/j.scitotenv.2023.164763.
72. Manono, B.O.; Mwami, B. Agroforestry and Soil Health: A Review of Impacts and Potential for Sustainable Agriculture. *J. Earth Sci*. **2026**, *7*, 31. https://doi.org/10.3390/earth7010031.
73. Kelvin, K.; Wahab, W.; Wulandari, M. Computer resource utilization analysis for Microsoft excel and python in data processing. *Eng. Math. Comput. Sci. J.* **2024**, *6*, 137–142. https://doi.org/10.21512/emacsjournal.v6i2.11736.
74. Naorem, A.; Jayaraman, S.; Dang, Y.P.; Dalal, R.C.; Sinha, N.K.; Rao, C.S.; Patra, A.K. Soil constraints in an arid environment—Challenges, prospects, and implications. *Agronomy* **2023**, *13*, 220. https://doi.org/10.3390/agronomy13010220.
75. Muhammad, M.; Waheed, A.; Wahab, A.; Majeed, M.; Nazim, M.; Liu, Y.H.; Li, L.; Li, W.J. Soil salinity and drought tolerance: An evaluation of plant growth, productivity, microbial diversity, and amelioration strategies. *Plant Stress* **2024**, *11*, 100319. https://doi.org/10.1016/j.stress.2023.100319.